Copper removal using a lump of clay from wastewater in central Côte d'Ivoire

ABSTRACT

Heavy metals such as copper are not only a problem for air pollution: they are bio persistent, disrupt ecosystems, damage soils, surface waters, forests, and crops, and accumulate in the food chain. The aim was to propose effective methods for quantifying and decontaminating wastewater containing copper. In this study, the treatment of copper(II)-containing wastewater was carried out using clay, and the concentration of Cu^{2+} was monitored using the differential pulse anodic dissolution voltammetry method. Physical characterization revealed the porous nature of our clay. Furthermore, the kinetic study of Cu^{2+} adsorption on clay is adapted to the pseudo-order 2 kinetic model, and the appropriate isotherm is that of Langmuir with an equilibrium time of 20 min. Cu^{2+} adsorption is maximal at pH = 6. The maximum monolayer adsorption capacity was found to be 66.54 mg/g.

Keywords: Voltammetry, copper, clay, adsorption

1. INTRODUCTION

"The rising levels of trace metals being discharged into the environment as industrial waste represent a serious threat to human health, life, resources and ecological systems. Although there are many sources of heavy metals, certain industrial sectors are currently the biggest contributors to environmental pollution by these toxic metals" [1]. Heavy metals are not biodegradable and tend to accumulate in living organisms, causing various disorders and diseases. Copper is one such metal. Although this element is essential for living organisms, acute doses cause certain health disorders in humans, including anemia, osteoporosis, hypoglycemia, arthritis, heart rhythm disorders and neurological problems [2, 3]. Excess copper can also damage lipids, nucleic acids and proteins [4]. Consequently, effluents containing Cu^{2+} from various industries require treatment before discharge into water.

There are several treatment methods that contribute to their elimination, such as ion exchange, reverse osmosis and activated carbon treatment [5], but the least costly remains adsorption on natural clay [6,7, 8]. Clays are characterized by their ability to adsorb metals and organic substances from aqueous solutions [9]. This property is essentially due to their natural acidity and high specific surface areas. Kaolin from the Katiola region belongs to this category of solids. Its abundance means that it is currently used in pottery by the potters of Katiola (a town in central Côte d'Ivoire). So our aim is to remove copper from wastewater using clay from the Katiola region.

2. MATERIAL AND METHODS

2.1 Clay activation

100 mL of hydrochloric acid (HCl) is added to 5 g of clay and stirred for 24 hours. Then decant and filter. Dry in an oven at 60°C for 24 hours. The clay is washed with distilled water to a neutral pH and then dried again for 24 hours.

2.2 Analytical methods for collected samples

The analytical method used to assess electrolysis performance in this work was a differential pulse voltammetry method, which enabled the evolution of paracetamol concentration to be determined from a pre-established calibration curve. This method also enables us to qualitatively detect the production of intermediates during treatment. Fig. 1 shows the different voltammograms obtained with different concentrations of copper (II) ions introduced into the reaction medium. These curves were obtained using parameters identical to those for Lead (deposit potential = -1.4 V, deposit time = 300 s, cleaning potential =1.4 V, cleaning time = 400 s, modulation amplitude = 30 mV, Modulation time = 30 ms, potential step = 4 mV, Time interval = 0.1 s) [10]

The voltammograms shown in Figure 1a were used to plot the calibration line for our concentration range. Figure 1b shows the calibration line for the chosen concentration range. This curve gives a determination coefficient R^2 = 0.998, which is very close to 1, and its equation is $I_{pic} = 7.10^{-07}$ $[Cu^{2+}] - 6.10^{-07}$. All these observations demonstrate the good linearity of the method.

The calibration curve was used to monitor the concentration of Cu^{2+} as it adsorbed onto the clay. During adsorption, samples of the reaction mixture were taken and the differential pulse anodic redissolution voltammeter curve of each sample was measured. The peak current intensity of each sample was determined. The concentration of Cu^{2+} in each sample was then determined using the calibration line obtained.

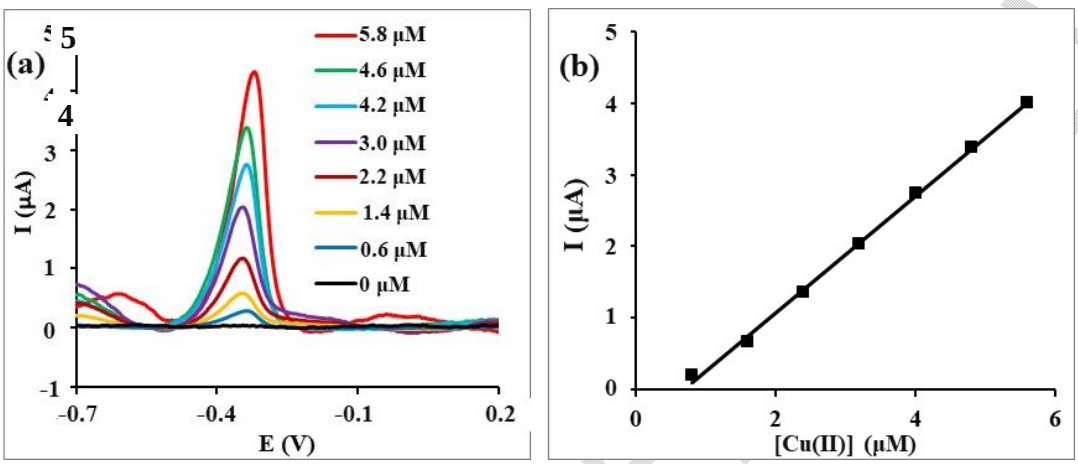

Fig. 1. (a) Differential pulse anodic redissolution voltammogram of different Cu^{2+} concentrations, T = 25°C, WE: BDD, CE: Pt, RE: MSE; (b) Method calibration curve

2.3 Adsorption rate

The adsorption rate (% adsorption) of copper on clay is obtained using the following formula:

$$\text{Adsorption rate (\%)} = \frac{(C_0 - C_t)}{C_0} \times 100 \quad (1)$$

With Co: initial copper concentration (mg/L); Ct: residual copper concentration at equilibrium (mg/L)

3. Results and discussion

3.1 Clay characterization

3.1.1 Scanning electron microscopy (SEM)

Fig. 2 shows a micrograph of the clay. This image shows the organization of the particles in the form of agglomerates of clay particles with irregular morphology.

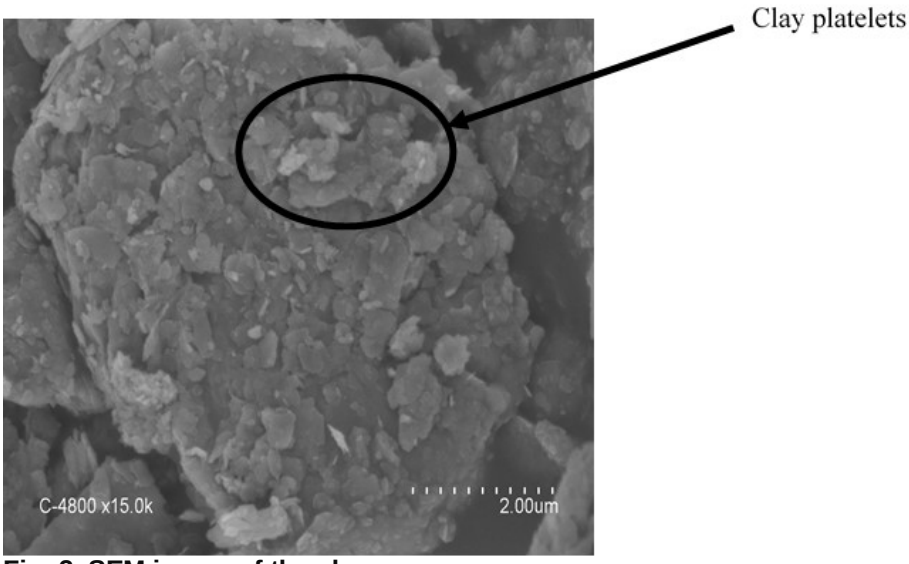

Fig. 2. SEM image of the clay

3.1.2 Specific surface

The specific surface area was determined using the Brunauer-Emmett-Teller (BET) multipoint method Brunauer [11]. A value of 56.7806 m^2/g was obtained with our clay. This shows that the clay is porous.

3.2 Elimination of Cu^{2+} by clay

3.2.1 Kinetics of Cu^{2+} adsorption by clay

The influence of agitation time on copper ion adsorption was studied. The results are shown in Fig. 3, where it is clear that the adsorption rate of Cu^{2+} increases with time up to 20 min. This stage corresponds to Cu^{2+} adsorption on the active sites of the clay. After 20 minutes, the adsorption rate remains constant at 70.73%. This indicates saturation of the clay pores [9, 12, 13]. A time of 20 min was therefore used as the equilibrium time for the remainder of our study.

In order to determine which kinetic model best describes Cu^{2+} adsorption on clay, the first-order pseudo-reaction and second-order pseudo-reaction models were applied, using equations 2 and 3 respectively [14, 15].

$$\ln(q_e - q_t) = \ln q_e - k_1 t \quad (2)$$

$$\frac{t}{q_t} = \frac{1}{k_2 q e^2} + \frac{1}{q_e} t \quad (3)$$

Where q_e and q_t are respectively the quantity of copper ions adsorbed per mass of clay at equilibrium and time t in (mg/g); k_1 (1/h) and k_2 ($g.mg^{-1}.h^{-1}$) are the adsorption rate constants.

The curves plotted are respectively $\ln(q_e - q_t)$ versus time and t/q_t versus time. The results obtained are shown in Fig. 4. Rate constants and linear determination coefficients are given in Table 1.

The results in Table 1 show that the determination coefficient are 0.965 and 0.999 for the pseudo-1-order and pseudo-2-order models respectively, indicating that the kinetic model that best describes the adsorption of copper ions onto clay is the pseudo-2-order model. The maximum experimental amount of Cu^{2+} adsorbed per clay mass (q_e) at equilibrium was determined to be 52.8 mg/g. Theoretical maximum values for the amount of copper ions adsorbed were also determined using the pseudo-order 1 and pseudo-order 2 kinetic models. Values of 9.48 and 53.19 mg/g were obtained for the pseudo-order 1 and pseudo-order 2 models respectively. These results show that the experimental value (52.8 mg/g) of the maximum amount of Cu^{2+} adsorbed is close to the theoretical value (53.19 mg/g) obtained by applying the pseudo-order 2 kinetic model. Thus, the kinetic model adapted to our study is the pseudo-order 2 kinetic model.

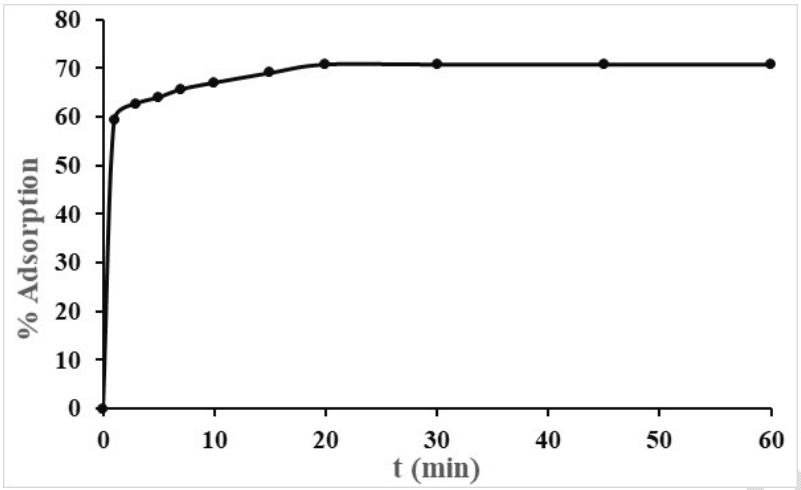

Fig. 3. Cu^{2+} removal efficiencies on clay; clay mass = 3 g; 50 mg/L Cu^{2+}; T = 25°C

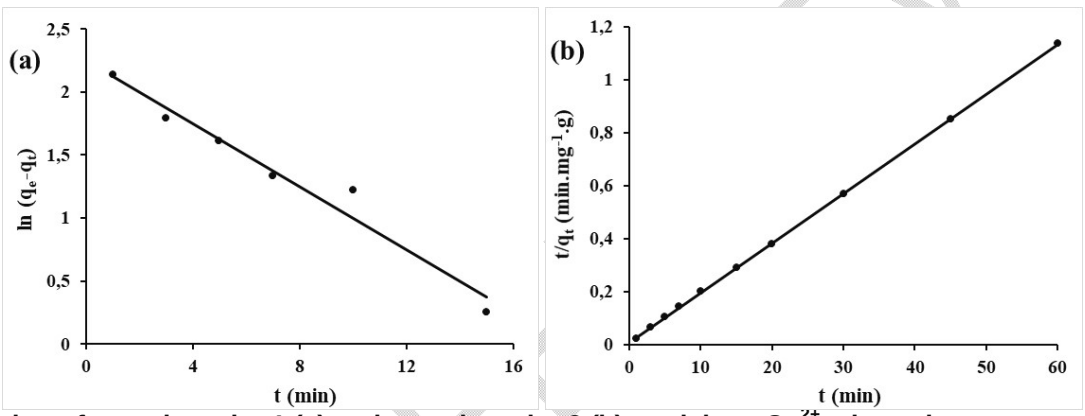

Fig. 4. Application of pseudo-order 1 (a) and pseudo-order 2 (b) models to Cu^{2+} adsorption

Table 1. Parameters for Cu^{2+} adsorption kinetics models

pseudo-order 1			pseudo-order 2		
k_1 (min^{-1})	R^2	q_{th}(mg/g)	k_2 ($g.mg^{-1}.min^{-1}$)	R^2	q_{th}(mg/g)
0,125	0,965	9,48	0,041	0,999	53,19

3.2.2 Influence of clay mass on Cu^{2+} adsorption

"The influence of clay mass was studied with the aim of determining the clay mass corresponding to an optimum adsorption rate of Cu^{2+}". [22] Fig. 5 shows the results obtained. In this figure, a rapid evolution of the adsorption rate can be seen when the clay dose varies from 0.05 g to 0.3 g in 50 mL of copper ions at a concentration of 50 mg/L. The adsorption rate for this dose variation increases from 13.4% to 70.75%. Above 0.3 g, the Cu^{2+} adsorption rate remains constant. Above 0.3 g of clay, the number of accessible free sites becomes stable. The addition of clay adds to the number of free sites, but these additional additions lead to the formation of agglomerations of clay particles, and exclude certain clay particles from the adsorption process [16].

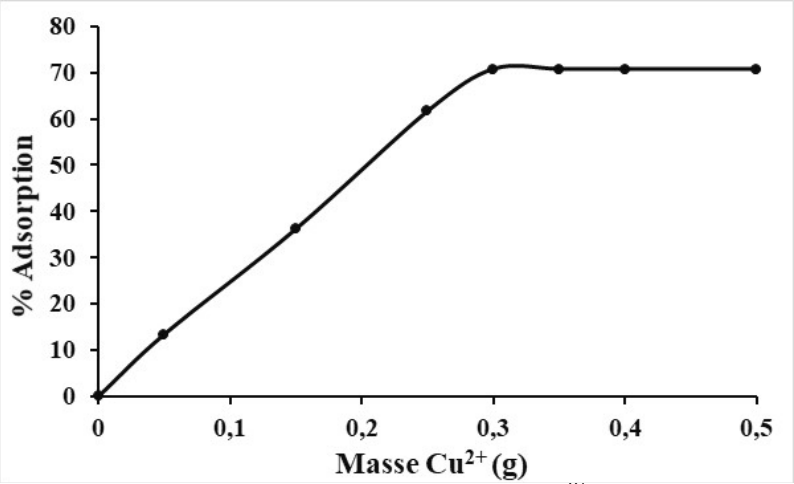

Fig. 5. Influence of adsorbent mass on Cu^{2+} adsorption

3.2.3 Adsorption isotherms

The empirical relationship for the Freundlich isotherm is of the form [12, 17, 18]:

$$q_e = K_f C_e^{1/n} \quad (4)$$

With :
q_e : Adsorption capacity in mg of adsorbed solute per g of adsorbent,
C_e: Equilibrium concentration of solute in the liquid phase (mg/L),
1/n and K_f: Adsorption coefficient and constant respectively.

The Freundlich constant (K_f) reflects the adsorption capacity of a matrix with respect to the adsorbent under consideration. The higher the value of K_f, the greater the adsorption. The linear transform used to verify the validity of equation (5) is obtained by logarithmic scaling:

$$\ln q_e = \ln K_f + \frac{1}{n} \ln C_e \quad (5)$$

If the graphical representation of *ln* q_e as a function of *ln* C_e yields a straight line, we can conclude that the Freundlich equation is applicable. This allows us to calculate the constants k and n [12].

The Langmuir model can be used to calculate the maximum adsorption capacity of adsorbent materials [14, 15, 19]. The Langmuir model is represented mathematically by the following equation:

$$q_e = \frac{q_m b C_e}{1 + b C_e} \quad (6)$$

Linearization of equation (6) yields:

$$\frac{1}{q_e} = \frac{1}{q_m} + \frac{1}{q_m b} \times \frac{1}{C_e} \quad (7)$$

With *b* the Langmuir thermodynamic constant related to the free energy of adsorption, q_e (mg/g) the quantity of solute adsorbed per unit mass of adsorbent at equilibrium and q_m (mg/g) the quantity of solute adsorbed per gram of solid required to cover the adsorbent surface with a monomolecular layer, or the maximum adsorption capacity. This (mg/L) represents the residual solute concentration at equilibrium.

The slope of the plot of $1/q_e$ versus $1/C_e$ is used to calculate the constants q_m and b.
Applied to our experimental results, the Freundlich and Langmuir models give fig. 6. The parameters obtained are shown in Table 2.

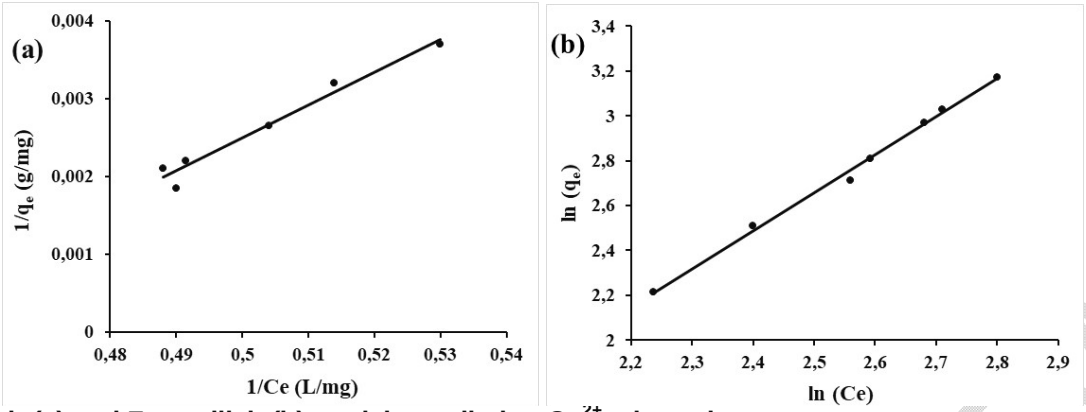

Fig. 6. Langmuir (a) and Freundlich (b) models applied to Cu^{2+} adsorption

Table 2. Parameters of the Langmuir and Freundlich equations

Freundlich			Langmuir		
R^2	ln K_f	N	R^2	q_m(mg/g)	B
0.967	1.582	0.589	0,995	66.540	0.355

Both models are applicable, but the Langmuir model describes this adsorption better, as its determination coefficient is closer to 1. This shows that the sites are equivalent (uniform surface), a monolayer is formed and there is no interaction between the adsorbed ions [12]. The maximum Cu^{2+} adsorption capacity of this clay is 66.54 mg/g.

3.2.4 Influence of pH on adsorption

pH plays an important role in adsorption kinetics. Previous studies [20] have shown that it is the main parameter that significantly influences the adsorption of metals onto clays. This is because the pH of the solution generally leads to a change in the surface charge of the adsorbent and also influences solute dissociation [16, 21].

The evolution is controlled as a function of time, i.e. 20 min agitation for each sample. The pH was adjusted with 0.1 N sodium hydroxyl and 0.1 N hydrochloric acid. The results obtained are shown in Fig. 7. The adsorption rate increases with pH from 1 to 6, then decreases slightly above pH 6. This shows that the maximum adsorption rate is obtained at pH 6.

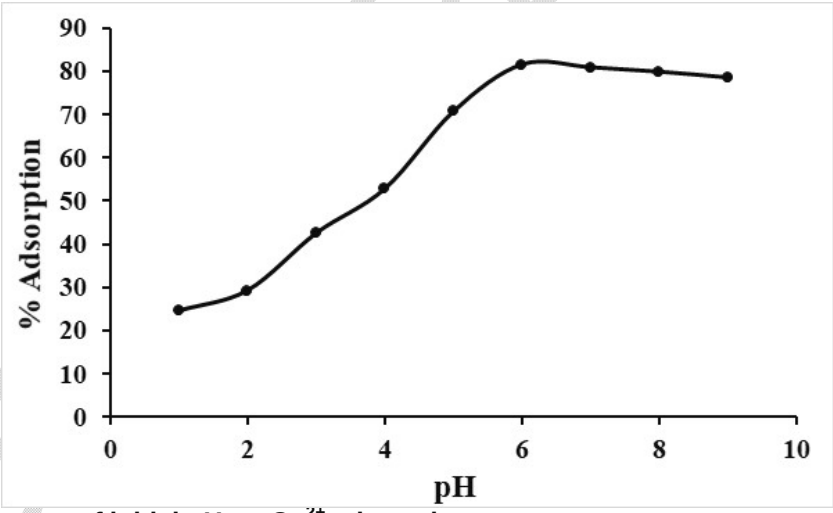

Fig. 7. Influence of initial pH on Cu^{2+} adsorption

4. CONCLUSION

The voltammetric study of copper oxidation in nitric acid media on the boron-doped diamond anode showed good linearity between oxidation peak current intensity and Cu^{2+} concentration (R^2=0.999). The differential pulse anodic dissolution voltammetric method enabled us to efficiently monitor Cu^{2+} concentration during adsorption onto clay. The kinetic study of Cu^{2+} adsorption on clay showed that the kinetic model suitable for our study is the pseudo-order 2 kinetic model with 20

min as equilibrium time. Equilibrium adsorption revealed that the experimental data best fit the isothermal Langmuir model. Cu^{2+} adsorption is maximal at pH = 6. The maximum monolayer adsorption capacity was found to be 66.54 mg/g.

REFERENCES

1. Alvarez-Ayuso E, Garcia-Sanchez A, Querol X. Purification of metal electroplating waste waters using zeolites. Water Research. 2003; 37: 4855–4862.
2. Mehta R., Templeton DM, O'Brien PJ. Mitochondrial involvement in genetically determined transition metal toxicity: II. Copper toxicity. Chemico-Biological Interactions. 2006; 163: 77–85.
3. Mohan D, Pittman CU, Steele PH. Single binary and multi-component adsorption of copper and cadmium from aqueous solutions on Kraft lignin a biosorbent. Journal of Colloid and Interface Science. 2006; 297: 489–504.
4. Halliwell B, Gutteridge JM. Role of free radicals and catalytic metal ions in human disease: an overview. Methods in Enzymology. 1990; 186: 1–85
5. Majdan M, Maryuk O, Plaska AG, Pikus S, Kwiatkowski R. Spectral characteristics of the bentonite loaded with benzyldimethyloctadecylammonium chloride, hexadecyltrimethylammonium bromide and dimethyldioctadecylammonium bromide. Journal of Molecular Structure. 2008; 874: 101–107.
6. Sdiri AT, Higashi T, Jamoussi F. Adsorption of copper and zinc onto natural clay in single and binary systems. Int. J. Environ. Sci. Technol. 2014; 11: 1081–1092. https://doi.org/10.1007/s13762-013-0305-1
7. Lidiany MZ, Zuy MM, Maria das GC, Wilder DS, João GM, Sara SV, David LN. Natural clay and commercial activated charcoal: Properties and application for the removal of copper from cachaça. Food Control. 2015; 47: 536-544. https://doi.org/10.1016/j.foodcont.2014.07.035
8. Vengris T, Binkien R, Sveikauskait A. Nickel, copper and zinc removal from waste water by a modified clay sorbent. Applied Clay Science. 2001; 18(3–4):183-190. https://doi.org/10.1016/S0169-1317(00)00036-3
9. Bintou C, Lemeyonouin AGP, Ollo K, Lébé PSK, Hervé G-D, Donourou D, Lassiné O. Valorization of Green Clay from Bouaflé (Ivory Coast) in the Simultaneous Elimination of Organic Pollutants and Metallic Trace Elements by Adsorption: Case of Methylene Blue and Cadmium Ions. Chemical Science International Journal. 2020; 29(8): 37-51.
10. Koffi KS, Kambiré O, Kouadio KE, Kimou KJ, Ouattara L. Detection of Lead (II) on a Boron-doped Diamond Electrode by Differential Pulse Anodic Stripping Voltammetry. Chemical Science International Journal. 2021; 30(7): 33-46.
11. Brunauer S, Emmett PH, Teller E. Adsorption of gases in multimolecular layers. J. Am. Chem. Soc. 1938; 60 (2): 309–319.
12. Abollé A, Kouakou YU, Kambiré O, Koné YT, Kouakou AR. Adsorption of Methyl Orange on Corncob Activated Carbon: Kinetic, Equilibrium, and Thermodynamic Studies, Earthline Journal of Chemical Sciences. 2022; 8(2): 205-224.
13. Kouakou YU, Kambiré O, Kouakou KKG, Trokourey A. Study of Potential Adsorption of Glyphosate on Iron-textured Soil. American Journal of Applied Chemistry. 2021; 9(6): 207-214.
14. Kouakou YU, Kambire O, ZranVanh E-S. Properties of magnetic carbon base on Ricinodendronheudelotii and application in removal of methylene blue. Int. J. Adv. Res. 2023; 10(11): 440-453. http://dx.doi.org/10.21474/IJAR01/15688
15. Kambiré O, Kouakou YU, Kouyaté A, Sadia SP, Kouadio KE, Kimou KJ, Koné S. Removal of rhodamine B from aqueous solution by adsorption on corn cobs activated carbon, Mediterranean Journal of Chemistry. 2021; 11(3): 271-281. http://dx.doi.org/10.13171/mjc02112131596ollo
16. Kifuani KM, Mayeko AKK, Vesituluta PN, Lopaka BI, Bakambo GE, Mavinga BM, Lunguya JM. Adsorption d'un colorant basique, Bleu de Méthylène, en solution aqueuse, sur un bioadsorbant issu de déchets agricoles de Cucumeropsis mannii Naudin. International Journal of Biological and Chemical Sciences. 2018 ; 12(1) : 558-575.
17. Lébé PM-SK, Daouda K, Max RWM, Aliou GLP, Gaoussou C, Léon KK, Jonas YA-Y. Use of two clays from Côte d'Ivoire for the adsorption of methyl red from aqueous medium. Chemical Physics Letters. 2023 ; 810 : 140183.
18. N'guessan LBK, Abollé A, Adjoumani RK, Victor G, Albert T. Using Modified Activated Carbon to Remove Methylene Blue and Rhodamine B from Wastewater. American Journal of Physical Chemistry. 2023; 12(3): 30-40. doi: 10.11648/j.ajpc.20231203.11
19. Kouakou YU, Kambiré O, Eroi NS, Koné YT, Trokourey A. Kinetic and Thermodynamic Study of the Elimination of Remazol Black on Activated Carbon Based on Ricinodendron heudelotii Shells. Journal of Materials Science and Chemical Engineering. 2023; 11:1-20. https://doi.org/10.4236/msce.2023.119001
20. Celedon S, Quiroz C, Gonzalez G, Sotomayor TCM, Benavente E. Lanthanides–clay nanocomposites: Synthesis, characterization and optical properties. Materials Research Bulletin. 2009; 44 (5): 1191–1194.
21. Wibowo N, Setyadhi L, Wibowo D, Setiawan J, Ismadji S. Adsorption of benzene and toluene from aqueous solution onto activated carbon and its acid heat treated forms: Influence of surface chemistry on adsorption. Journal of Hazardous Materials. 2007: 146; 237-242.
22. Abollé A, Urbain KY, Ollo K, Tchonrontcha KY, Rodrigue KA. Adsorption of Methyl Orange on Corncob Activated Carbon: Kinetic, Equilibrium, and Thermodynamic Studies. Earthline Journal of Chemical Sciences. 2022 Aug 4;8(2):205-24.